PERGAMON

Acta mater. Vol. 47, No. 9, pp. 2821–2829, 1999

Printed in Great Britain
PII: S1359-6454(99)00120-2
1359-6454/99 $20.00 + 0.00

EXCESS ENERGY OF GRAIN-BOUNDARY TRIJUNCTIONS: AN ATOMISTIC SIMULATION STUDY

S.G. SRINIVASAN†[1]‡, J.W. CAHN[2], H. JÓNSSON[3] and G. KALONJI[1]

[1]Department of Materials Science and Engineering, University of Washington, Seattle, WA 98195, U.S.A., [2]National Institute of Standards and Technology, Gaithersburg, MD 20899, U.S.A. and [3]Department of Chemistry, University of Washington, Seattle, WA 98195, U.S.A.

(Received 18 December 1998; received in revised form 26 March 1999; accepted 26 March 1999)

Abstract—Atomic-scale computer simulation was used to study grain-boundary trijunctions, which are defined as the intersection of three grain boundaries. The simulation system consisted of a three-dimensional periodic array of columnar f.c.c. grains having three different orientations with a common [001] direction, and in which all grains are rotated 30° from their neighbors. The inter-atomic interactions were described by the Lennard–Jones potential. Each simulation cell contained six trijunctions plus the nine associated symmetric tilt grain boundaries. The energy of systems of differing sizes was monitored during annealing and after quenching to obtain quantitative estimates of the excess energy of the grain boundaries and trijunctions. For this system, the total excess energy contributed by the trijunctions was found to be negative. This result is consistent with recent calorimetry experiments on high-purity nanocrystalline cobalt conducted elsewhere.

1. INTRODUCTION

Trijunctions (TJs), also called triple junctions, are lines along which three phases or grains meet. More rigorously, they are the lines of intersection of the three surfaces or interfaces between these phases or grains. At an atomistic level, trijunctions have a structure that is easily discernible as three-dimensional. Trijunctions play important roles in determining a variety of material properties. In this work, we use atomistic computer simulations to demonstrate that the excess energies of grain-boundary trijunctions can be negative. This finding is expected to have consequences for nanostructural stability and for grain-growth kinetics at small length scales.

The notion of negative trijunction excess energy is counterintuitive. According to McLean, "just as atoms along a grain boundary interface are in positions of higher free energy than those inside a grain, so the atoms at grain boundary junctions, being under the influence of three instead of two competing forces, are in positions of still higher free energy" [1]. This has been taken to imply that the excess line energies of triple junctions must always be positive [2]. Although Gibbs showed that excess surface free energies (per unit area) had to be positive, he discussed the possibility that the excess free energy of a trijunction among fluid phases, which he termed *line tension*, could be negative [3].

Fortier *et al.* [2] used scanning–tunneling microscopy to estimate TJ excess energy by looking at grain-boundary groove depths in the vicinity of a trijunction–free surface intersection. For their analysis they assumed that: (a) grain boundaries intersect at 120°; (b) interfacial torque is zero; (c) TJ excess energy is a constant; and (d) the grain-boundary groove angles and groove depths were constant. Representing the local geometry at a thermally etched junction as irregular tetrahedra, they related the ratio "q" of the trijunction depth (z_t) and the grain-boundary groove depth (z_b) as a function of grain-boundary, free-surface and trijunction energies. For a system with grain-boundary to surface energy ratio of 0.3, they argued that the groove depth at a trijunction should be 33% deeper ($q = 1.33$) than the adjoining grain-boundary groove even when trijunction excess energy is zero. They observed that some junctions had $q \gg 1.33$ and attribute the positive deviations to positive TJ excess energy.

Trijunctions in fluid systems have been extensively examined from many different viewpoints. Materials scientists trying to understand grain growth in metals have used the coarsening behavior of soap froths as an analogy [4]. The influence of trijunctions and the behavior of their line tensions near a wetting phase transition have evoked considerable interest in the statistical mechanics community [5–7]. Such studies were undertaken to

†Now at the Los Alamos National Laboratory, New Mexico, U.S.A.
‡To whom all correspondence should be addressed.

obtain insight into fluid dispersions because of their practical relevance to oil and mineral recovery processes. The line tension of trijunctions in wet soap froth can be easily shown to be negative (see Appendix A for a detailed derivation). However, using a free-energy minimization procedure and assuming a positive line tension, Morgan and Taylor [8] have solved for the equilibrium configuration of a tetrahedral point junction (where four grains meet) in a soap-froth-like system. In their model, they added an additional TJ excess energy term, associated with a *mathematically sharp line*, to the total surface free energy. They found the system minimized its energy by reducing the network length, and in the process split the tetrahedral point junction into two trijunctions. They argued that there is no solution if the line tension is negative. It is important to remember that in most polycrystalline systems, one cannot get mathematically sharp trijunction lines.

For trijunctions among three fluid phase systems, the structure and properties depend only on the phases present and on state variables, such as the temperature, chemical potentials, and the imposed pressure. On the other hand, additional geometrical variables are required to describe TJs that involve crystalline phases. Analogous to the five angles that need to be specified for a planar grain boundary, eleven angles are required to specify a grain boundary TJ. Due to such inherent complexities of polycrystalline materials, it has been difficult, both experimentally and theoretically, to isolate unambiguously the contributions of grain boundaries or TJs to material properties.

Tremendous advances occurred in the study of grain boundaries when Schober and Balluffi [9] created and studied individual planar grain boundaries in specially fabricated bicrystals. Although it is much harder to craft an equivalent study for trijunctions and higher order multi-junctions in solids, there has been some success [10]. Dahmen and coworkers [10] have studied polycrystalline Al thin films grown epitaxially on single-crystal Si (111) substrates. Only a limited number of Al grain orientations resulted because of the influence of the underlying substrate. The Al [001] directions of each grain are parallel to each other and to the [111] direction of the silicon substrate, while the other Al cubic axes lie parallel to the $[\bar{1}10]$ and $[11\bar{2}]$ directions of the silicon substrate. Each of the three cubic grains is thus related by rotations of 30° or, equivalently, 60°, 120° or 150° about a common [001] axis.

2. SIMULATION GEOMETRY

For our simulations, we tried to emulate the system of Dahmen and coworkers by contriving a *restricted* polycrystal in order to reduce the number of crystallographically distinct grain boundaries and TJs in our system. We used a molecular dynamics (MD) technique [11] to determine optimal atomic structures of the grain boundaries and trijunctions. Grain-boundary and trijunction excess energies were extracted by analyzing the dependence of the total excess energy on system size.

Although all TJs in our system are junctions of the same three grains, they belong to two different symmetry classes [12]. Furthermore, any two adjacent parallel TJs must belong to the two different classes. In the higher symmetry class, denoted *S*, for color *survival*, the highest possible two-dimensional point symmetry projected along [001] is 3*m*. There are two trijunctions in this class with symmetry 3 and one trijunction with point symmetry 3*m*. The three TJs in the lower symmetry class, denoted *C* for color *clash*, all have the highest projected symmetry of *m*. For our simulation geometry, we cannot construct a system with fewer than three TJ symmetries.

Two geometrical constructs, the *tri-chromatic* pattern and the *Y*-operator, are used to generate atomic configurations of various trijunctions belonging to the two classes *S* and *C*. The tri-chromatic pattern, for our system's geometry, consists of three inter-penetrating f.c.c. crystals related by rotations of 30° or, equivalently, 60°, 120° or 150° about a common [001] axis. To distinguish the starting crystal configuration from the two crystals that arise from rotation about the [001] axis, we assign a unique color to each of the three crystals (e.g. blue, red and green, respectively). A tri-chromatic pattern is shown in Fig. 1. Here, instead of colors, we use open or closed circles and squares to denote atoms in the three crystals. Clearly, two types of symmetry operations exist: (a) *classical* symmetry operations that transform a crystal of a given color into itself; and (b) *color* symmetry operations, for which geometrical transformations are combined with color permutations. For example, the "blue" mirrors illustrated in Fig. 1, denoted by plain lines, transform blue crystal into itself, while transforming red and green crystals into each other and flipping colors. The *Y*-operator consists of three arms that are separated by angles of 120° each. To generate a trijunction with desired point symmetry, we first place the origin of the *Y*-operator arm at the center of our tri-chromatic pattern. Next, we rotate the *Y*-operator to align its arms along the desired symmetry elements of the three-color object. Finally, we retain only points of one color (and discard points with the other two colors) in the region between two adjacent arms of the *Y*-operator. The *S* and *C* class trijunctions with symmetry 3*m* and *m* are illustrated in Fig. 2.

There is a variety of ways to construct a three-dimensional periodic system of grains with alternating classes of trijunctions. The system we used in our simulations had a space group $P\bar{6}m2$, or $p31m$ in two-dimensional projected symmetry, and is illus-

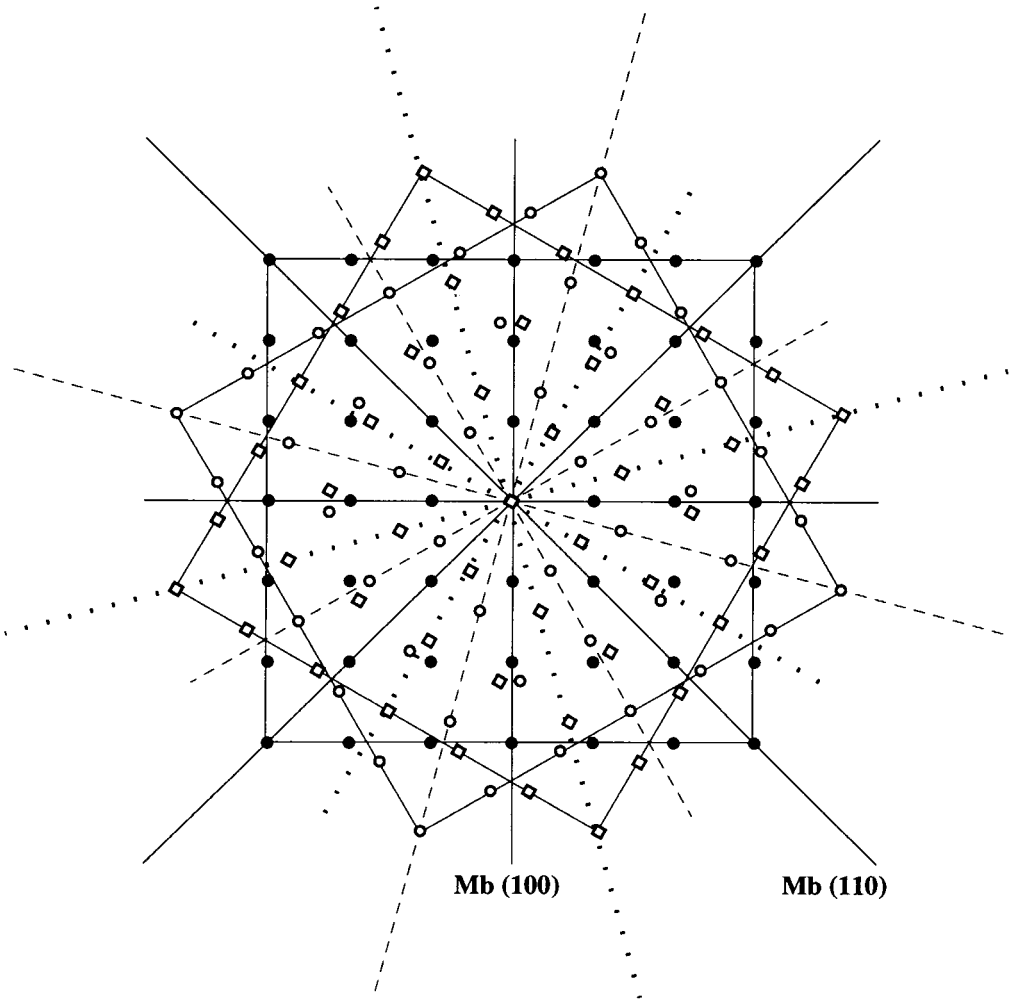

Fig. 1. The starting tri-chromatic pattern (also called the three-color object) from which trijunction configurations are generated. The [001] rotational axis passes through the center of the pattern. Only atoms in the bottom two layers are shown. Atoms in the three crystals are shown by different symbols (closed circles denote blue, open circles denote red and open squares denote green atoms).

trated in Fig. 3. In that arrangement, any two neighboring vertices of the three-color hexagonal grid are trijunctions belonging to the two different classes (marked *S* and *C* in the figure). The atomic configuration for such a system is generated as follows. The 3*m* trijunction vertex of the hexagonal grid is first placed on top of the center of the three-color object. Next, the grid as a whole is rotated to align it in accordance with the desired symmetry directions in the three-color object. Only blue-colored atoms are retained inside the blue hexagons, red atoms inside red hexagons and so on. For our simulations, we retain only atoms within the rhomboidal boxes marked in the figure.

3. MOLECULAR DYNAMICS METHOD

Molecular dynamics simulations are restricted by available computer power to the study of nanoscale system sizes evolving over nanosecond timescales. Nevertheless, simulations carried out with carefully designed bicrystal and polycrystalline systems can give valuable atomistic insight. We have used a parallel implementation of molecular dynamics for our simulations [13, 14]. The MD method involves the determination of the atomic trajectories by numerically solving Newton's equations of motion of a system of N interacting atoms [11]. A Lennard–Jones pair potential was used to describe the atomic interactions:

$$\phi(r_{ij}) = 4\varepsilon\left[\left(\frac{\sigma}{r_{ij}}\right)^{12} - \left(\frac{\sigma}{r_{ij}}\right)^{6}\right] \qquad (1)$$

This potential form was chosen for its computational simplicity.

We set the Lennard–Jones distance parameter (σ) and energy parameter (ε) equal to 1.0, and truncated the range of atomic interactions at 3σ. Five different system sizes, generated by increasing the separation between two neighboring trijunctions,

were studied. They corresponded to trijunction spacings of 11.04σ, 16.56σ, 22.08σ, 27.6σ, and 33.12σ. In all of these systems, the initial slab thickness was held constant at slightly over 2.5 times the cutoff distance of the interaction potential used for our simulations. This yields systems with 9560, 21 920, 39 350, 61 260 and 88 710 atoms, respectively.

The trijunction systems generated geometrically from the tri-chromatic pattern will have atoms at the grain boundaries that lie very close to each other. We performed a systematic study, with our smallest system size, to understand how the separation of pairs at the grain boundaries affects the system structure and energetics. We specified a variety of cutoff distances (r_c) to mark interfacial atom pairs as *close* pairs if their separation is less than r_c. One atom from each close pair is then removed from the system. The resulting system is then annealed and energy minimized to determine its cohesive energy. The cohesive energies were quite low for the cases where very small or large values were used for the cutoff distance (r_c). These two scenarios correspond to high repulsion when the chosen r_c is very small and to very low grain-boundary densities when the r_c used was very high. For a range of r_c values from $0.35a_0$ to $0.70a_0$, we obtained very similar cohesive energy for the annealed system, to within 0.1%. We used an r_c value of $0.56a_0$, where a_0 is the f.c.c. unit-cell parameter, to mark interfacial close pairs as this cutoff distance yielded the highest cohesive energy.

The simulation procedure involves equilibrating the system by annealing it at approximately two-thirds of its melting temperature (T_m) [15]. This provides mechanism(s) for relaxing the system to new lower energy configurations. The annealing process was carried out using the constant pressure molecular dynamics method of Parrinello and Rahman [16]. This method is an extension of Andersen's approach [15] to make it applicable to anisotropic systems such as crystalline solids. It allows the application of an arbitrary external stress to the simulation system. Treating the simulation box edge vectors as dynamical variables also permits both the shape and size of the simulation box to vary with time in response to the difference between the internal microscopic stress and the constant external stress. The Parrinello and Rahman technique is more effective in the study of solid–solid transformations than the constant volume mol-

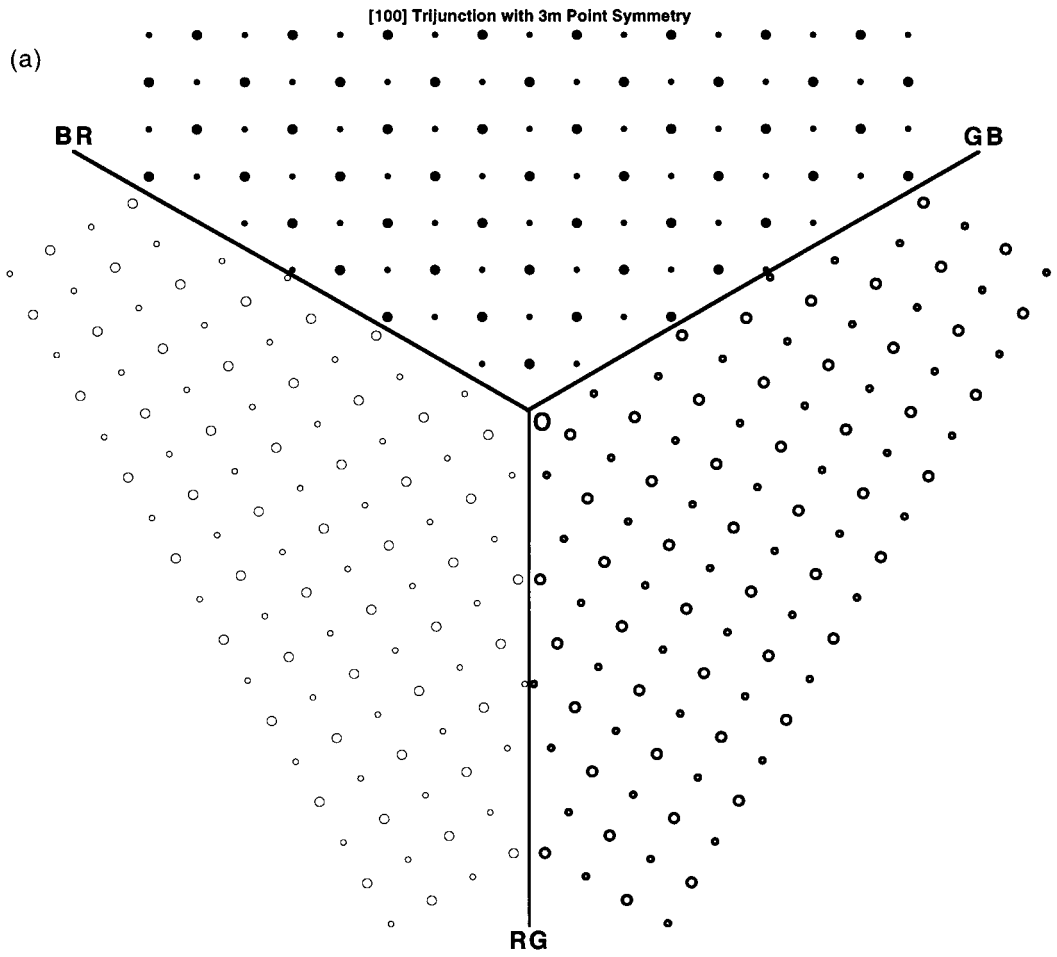

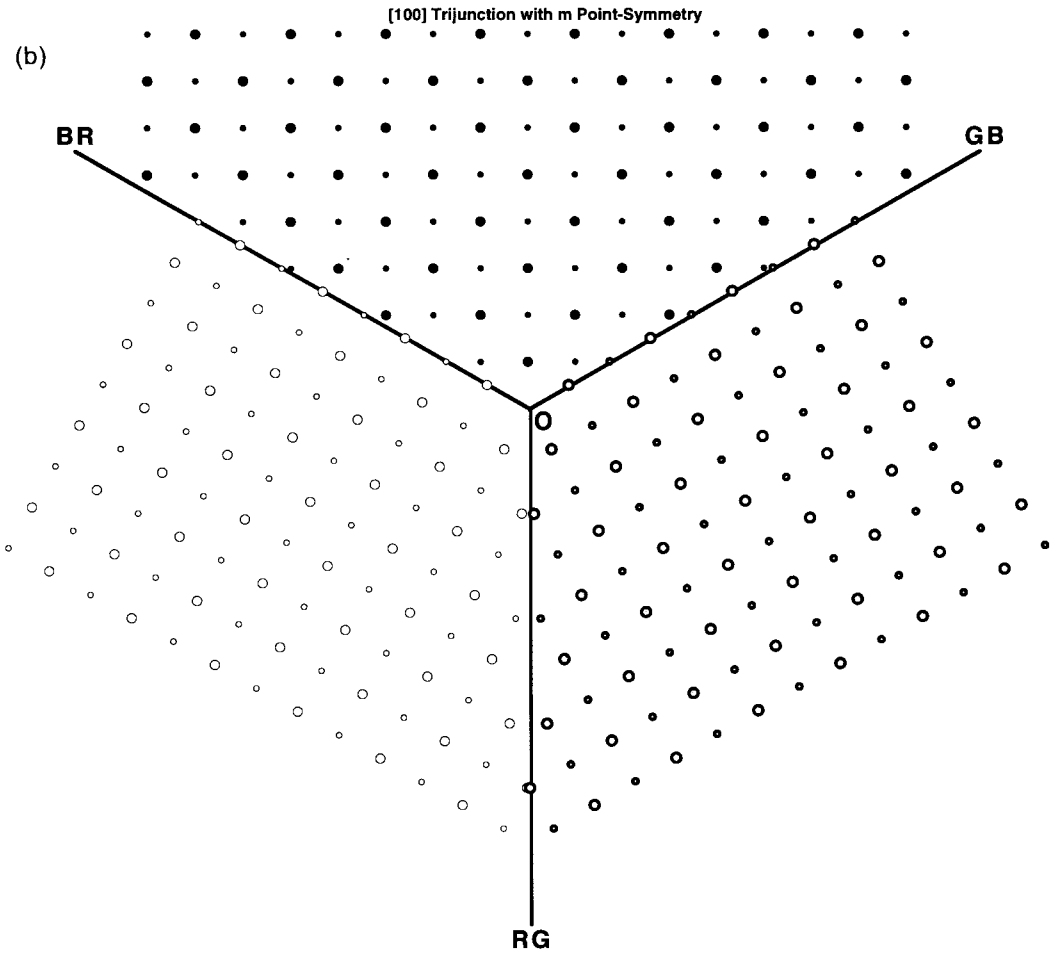

Fig. 2. An illustration of the symmetry of *S* and *C* class trijunctions. (a) (*facing page*) An *S* class trijunction with projected point symmetry 3*m* along [001]. (b) A *C* class trijunction with a projected symmetry *m* along [001]. The three grain boundaries are marked O-BR, O-RG, and O-GB. 3*m* symmetry denotes that the trijunction line is a three-fold rotational axis, and each of its three constituent grain boundaries are mirror planes that transform one crystal to its neighbor lying on the other side of the mirror. *m* symmetry indicates that only one of the three constituent grain boundaries is a mirror plane (O-RG). Only atoms in the bottom two layers are shown. Atoms in the three crystals are shown by different symbols (thin or thick bordered open circles and closed circles). Here, B, R and G, respectively denote blue, red and green crystals.

ecular dynamics method because shape and volume changes are not restricted.

We extracted GB and TJ excess energies for two different cases using a size dependence method described below. In the first case, we computed time-average excess energies at the finite annealing temperature, over the final 1000 time-steps of annealing. For the second case, we computed the excess energy of the system after quenching the annealed configurations to $T = 0$ using a steepest descent method. Annealing times for the simulations were determined by finding an annealing schedule that reduces CPU time and yet results in reasonably constant cohesive energy values. Towards this end, we annealed two smaller systems to 100 000 steps and plotted cohesive energy vs time. From these plots, we determined that annealing times of 10 000 to 15 000 steps were adequate for all our systems: 15 000 steps were used for the two larger systems. Subsequently, we performed longer annealing of larger systems for up to 70 000 time-steps to confirm that the cohesive energies had indeed equilibrated well.

4. METHOD FOR EXTRACTING GB AND TJ EXCESS ENERGIES

The geometry and dimensions of the simulated systems are shown in Fig. 4. There are three 30° and six 60° symmetric tilt GBs in our system with areas S_{30} and S_{60}, respectively, and six trijunctions each of length "*C*". For large enough systems, the total energy is:

$$E = VE_{\mathrm{v}} + \sum_{\text{three } 30^\circ \text{ GBs}} S_{30}\gamma_{30} + \sum_{\text{six } 60^\circ \text{ GBs}} S_{60}\gamma_{60} + \sum_{\text{six TJs } i} C\lambda_i \quad (2)$$

Here E_{v} is the energy per unit volume of single crystal, γ_{30} and γ_{60} are the excess energy per unit area of the 30° and 60° grain boundaries, and λ_{i} the excess energy per unit length of the trijunction "*i*". Rewriting equation (2) such that the terms on its right-hand side represent the total excess energy due to all of the system defects (GBs and TJs), we have:

$$E_{\mathrm{defects}} = E - VE_{\mathrm{v}} = E_{\mathrm{GB}} + E_{\mathrm{TJ}} \quad (3)$$

From the system geometry, the total GB excess energies can be written as:

$$E_{\mathrm{GB}} = \left(1.2679\gamma_{30} + 1.7932\gamma_{60}\right)AC = 3.0611\gamma_{\mathrm{mean}}AC \quad (4)$$

Similarly, grouping the six trijunction energies into λ_{total}, we have:

$$E_{\mathrm{TJ}} = \sum_{\text{six TJs } i} C\lambda_i = C\sum_{\text{six TJs } i} \lambda_i = 6C\lambda_{\mathrm{mean}} \quad (5)$$

Here, γ_{mean} is the average excess energy per grain boundary, and λ_{mean} is the average excess energy per trijunction. Using the above equations, we get an expression for total energy of defects per unit length of TJ as given in equation (6).

$$\frac{E_{\mathrm{defects}}}{C} = 3.0611\gamma_{\mathrm{mean}}A + 6\lambda_{\mathrm{mean}} \quad (6)$$

Thus, a plot of (E_{defects}/C) vs system sizes, A, should yield a straight line with *slope* $3.0611\gamma_{\mathrm{mean}}$ and *intercept* $6\lambda_{\mathrm{mean}}$. These are, respectively, the total GB and TJ excess energies. By this approach, one can unambiguously distinguish the contributions to the excess energy arising from the grain boundaries from those arising from the trijunctions. Values of the grain-boundary excess energies so obtained can be independently verified through separate bicrystal simulations. However, a limitation of this approach is that we obtain only the sums of excess energies over various classes of defects, e.g. the sum of the energies of the three different trijunction types.

5. RESULTS AND DISCUSSIONS

The total excess energy, computed with reference to that of a perfect single-crystal system, was plotted for five different systems as a function of their sizes. Two different cases were considered: (i) energies of systems that were annealed for 10 000 to 15 000 steps and then quenched to $T = 0$ using a steepest descent method; and (ii) energies of systems, all held at finite temperature for 20 000 steps. For the finite temperature systems, excess energies were averaged over the last 1000 time-steps of annealing. For the quenched systems, excess energies were computed for the final energy-minimized configurations. For each of these two cases, excess energy was plotted as a function of system size as shown in Figs 5(a) and (b). The slopes of these lines are the total excess surface energy of the nine grain boundaries, and are respectively, 2.449 and 2.733 in the Lennard–Jones ε/σ^2 units. The intercepts are the mean excess line energies of the six trijunctions, which were found to be negative, both at finite temperature and after quenching to $T = 0$. They are, respectively, −5.791 and −2.133 in ε/σ units. Recall there are three different trijunctions in our system, and that our technique only yields the sum of their contributions to the measured excess energy. Thus, at least *one* of the trijunctions must have a negative excess energy.

The energies of the 30° and 60° symmetric tilt GBs were determined from independent bicrystal simulations at $T = 0$ and $T = 2/3$ (T_{m}). For simulations at $T = 0$ we used standard lattice-statics simulations based on a Region-1–Region-2 formulation [18]. For the finite temperature case, the GB excess energies are time-averaged values obtained from simulations of the corresponding bicrystals using three-dimensional periodic boundary conditions. The values of GB excess energy for the $T = 0$ systems were lower than those obtained from the line-slope method by about 1%, while those for the finite temperature systems were lower by about 7%. Clearly, there is a good agreement of the GB energy values obtained from trijunction and bicrystal simulations.

When we say that trijunction excess energy is negative, it is important to clarify the frame of reference. We followed the Gibbsian procedures to compute excess quantities. Accordingly, we defined the excess energy due to grain boundaries as the difference between the computed energy of a unit cell of our bicrystal computation volume and the energy of a single crystal with the same number of atoms. We define the excess energy due to the TJs as follows: it is the difference between our computed energy for a unit cell of our polycrystalline computation volume and the sum of the energy of a single crystal with the same number of atoms plus the excess energy due to the grain boundaries present. Negative TJ energy implies that the excess energy in the vicinity of a TJ is less than it would have been for planar grain-boundary segments with areas equal to the areas of the three grain boundaries that would meet there if the TJ were *mathematically thin* lines. The energies of the atoms in grain boundaries are higher than the energies of atoms in a single crystal, and the energies of some atoms in TJs may be higher still, but they are not three times as high as the grain-boundary energy. In fact, our simulations show that some TJ atoms have lower energies than grain-boundary atoms.

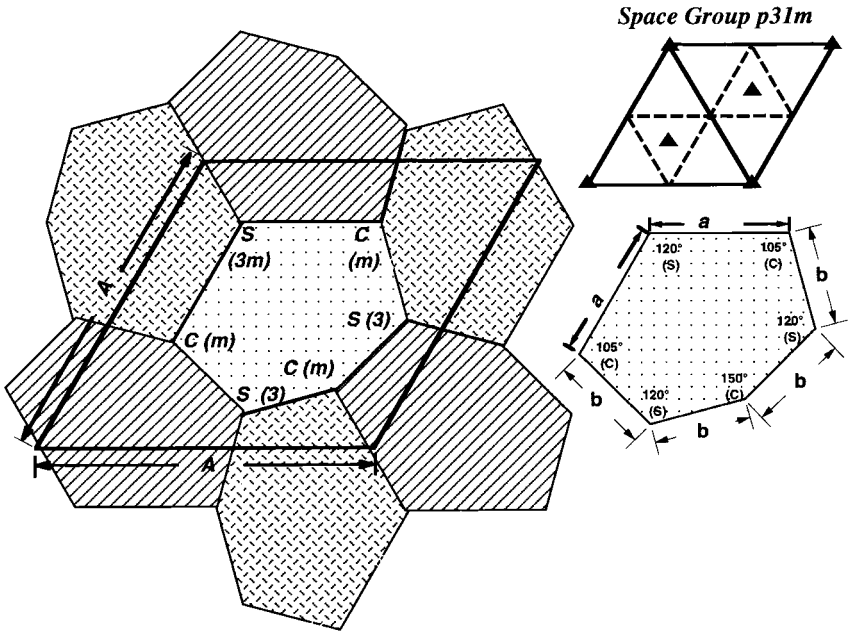

Fig. 3. Three-color tiling pattern used in simulations is shown along with its two-dimensional space group. Color *clash* and *survival* trijunctions are marked as *C* and *S*, respectively. Symmetries of the TJs are shown within parentheses. Edges of the hexagons are *a*–*b*–*b*–*b*–*b*–*a*, where $a = b\sqrt{2}$. The hexagon angles are 120°–105°–120°–150°–120°–105°. By our convention: the central hexagon is blue crystal, hexagons with hashed lines are red and hexagons with a mosaic pattern are green.

More detailed studies will be undertaken to explore this aspect.

McLean wrote of free energies per atom, but surely meant energies per atom. Chemical potentials—which are usually considered to be the free energies of atoms—at equilibrium are constant throughout the system, regardless of whether the atoms are in grains, at a TJ or GB. Our simulations determine energies, not free energies. This distinction is significant. The energies of grains and of grain boundaries rise with temperature, as we see in our simulation results, while the free energies of grains and, in single-component systems, of grain boundaries must decrease monotonically. In the ultimate analysis, it is conceivable that some TJs have positive energies. However, the inference that the excess energies of all TJs must be positive is not tenable.

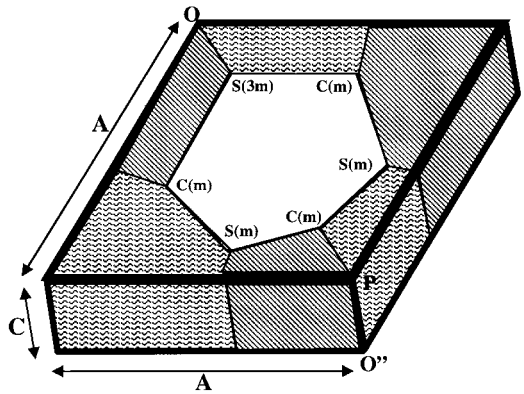

Fig. 4. Three-dimensional view of the periodic simulation box with the box dimensions marked. All the grains, except the central grain, are shaded differently to highlight their different orientations. The grain boundaries (GBS) meeting at the *S*(3*m*) trijunction, and *C*(*m*)-P and P-O″ are the 60° GBS. The remaining gbs, demarcated by black lines, are 30° boundaries. Thick black lines demarcate simulation box borders.

It is shown in Appendix A that the total energy of the system is lowered when there are wet trijunctions instead of dry ones. Evidently, for a given volume of fluid introduced into a trijunction, the energy decrease is proportional to the total junction length. To achieve this reduction, the trijunctions must be well separated and should possess large radii of curvature relative to the square root of the area of the liquid cross-section. For such systems, this energy reduction can be interpreted as effective negative line energy. At this juncture it is advisable to make a clear distinction between *diffuse-interface* models such as ours (that assume wet films at the interfaces) from *sharp-interface* models that assume positive surface energy and negative line energy. In *sharp-interface* models, using energy-minimization-based criteria for equilibrium or growth will not work when the trijunction energy is negative. This is because it is possible in that case to increment the surface areas by small amounts, and produce very oscillatory and infinitely long trijunctions. The total energy of this system would then approach minus infinity, a mathematically unsettling scenario [8].

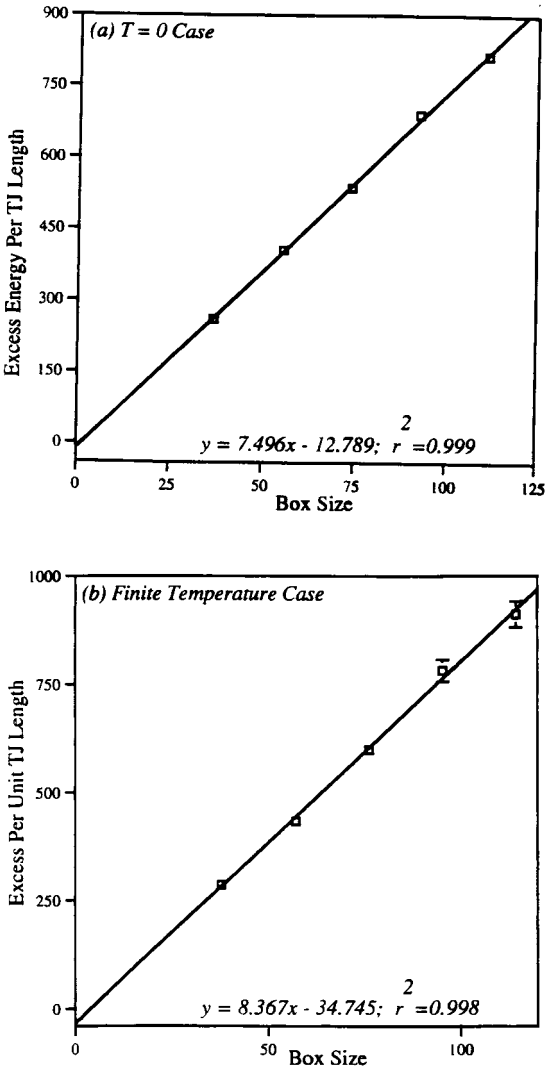

Fig. 5. Excess energy of the systems per unit length of the trijunctions plotted as a function of their size: (a) systems annealed and energy quenched to $T = 0$; and (b) systems annealed at finite temperature.

It may be argued that since the grain boundaries are regions of lower overall densities, it is necessary to use many-body interaction potentials to get reliable results for grain-boundary structure. It has been convincingly demonstrated, however, that pair-potentials yield grain-boundary structures similar to those obtained from potentials such as the embedded atom method (EAM) that incorporate many-body interactions [17, 18].

Recently, Hibbard and coworkers [19, 20] performed differential scanning calorimetry (DSC) experiments on 99.99% pure nanocrystalline cobalt possessing equiaxed grains with average grain sizes less than 100 nm. They observed a decrease in enthalpy and an increase in the DSC curve peak values at smaller grain sizes. Their data can be replotted, in terms of product of excess energy and square of the grain size as a function of grain size, to extract TJ energies. A straight line on such a plot reveals that the excess energy is given by just the two terms due to grain-boundary area and TJ line length, as in equation (2). The intercept of this plot is then the TJ excess energy, which was found to be negative. Hibbard and coworkers also found that the activation energy for grain growth increased with decreasing grain size.

6. CONCLUSIONS

Using atomistic computer simulations on a well-defined polycrystalline system, we have shown that trijunction excess line energies can be negative. This result has significant implications for materials properties, stability of nanostructures, and for microstructural evolution kinetics at small length scales where length effects dominate area effects. A systematic study is necessary for a fuller understanding of these implications. Grain-boundary excess energy independently assessed, through separate bicrystal simulations, agreed well with the values obtained through the system size-dependency analysis.

Acknowledgements—SGS acknowledges a graduate assistantship made possible by the Kyocera Chair at the University of Washington. HJ acknowledges partial support by NSF under Grant No. CHE-9217774. GK's work was partially funded by the Kyocera Chair at the University of Washington. We thank Branko Grunbaum and Richard Karp (University of Washington), and Jean Taylor (Rutgers University) for helpful discussions. Simulations were carried out on SP2 donated by IBM to the University of Washington.

REFERENCES

1. McLean, D., *Grain Boundaries in Metals*. Clarendon Press, Oxford, 1957, p. 49.
2. Fortier, P., Palumbo, G., Bruce, G.D., Miller, W.A. and Aust, K.T., *Scripta metall.*, 1991, **25**, 177.
3. Gibbs, J.W., *Trans. Connect. Acad. Arts Sci.*, 1874, **3**, 289.
4. Weaire, D. and Rivier, N., *Contemporary Phys.*, 1984, **25**, 59.
5. Rowlingson, J.S. and Widom, B., *Molecular Theory of Capillarity*. Clarendon Press, Oxford, 1982.
6. Indekeu, J.O., *Int. J. Mod. Phys. B*, 1994, **8**, 309.
7. Dussaud, A. and Vignes-Adler, M., *Langmuir*, 1997, **13**, 581.
8. Morgan, F. and Taylor, J.E., *Scripta metall. mater.*, 1991, **25**, 1907.
9. Schober, T. and Balluffi, R.W., *Phil. Mag.*, 1969, **20**, 511.
10. Thangaraj, N., Westmacott, K.H. and Dahmen, U., *Appl. Phys. Lett.*, 1992, **61**, 913.
11. Allen, M.P. and Tildesley, D.J., *Computer Simulation of Liquids*. Clarendon Press, Oxford, 1987.
12. Cahn, J.W. and Kalonji, G., *J. Phys. Chem. Solids*, 1994, **55**, 1017.
13. Srinivasan, S.G., Ashok, I., Jónsson, H., Kalonji, G. and Zahorjan, J., *Comput. Phys. Commun.*, 1997, **102**, 28.
14. Srinivasan, S.G., Ashok, I., Jónsson, H., Kalonji, G. and Zahorjan, J., *Comput. Phys. Commun.*, 1997, **102**, 44.

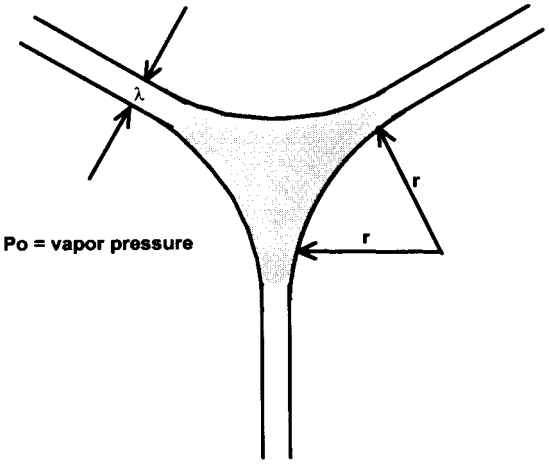

Fig. 6. An illustration of a trijunction line formed by three soap bubbles.

15. Andersen, H.C., *J. Chem. Phys.*, 1980, **72**, 2384.
16. Parrinello, M. and Rahman, A., *J. appl. Phys.*, 1981, **52**, 7182.
17. Vineyard, G.H., in *Battelle Colloquium*, ed. P.C. Gehlen, J.R. Beeler and R.I. Jaffee. Plenum Press, New York, 1972, p. 3.
18. Daw, M.S., Foiles, S.M. and Baskes, M.I., *Mater. Sci. Reports*, 1993, **9**, 251.
19. Hibbard, G., M. Sc. Thesis, University of Toronto, 1998.
20. Hibbard, G., Erb, U. *et al.*, in Proc. Canadian Metal Physics Conf., Kingston, Ontario, 1998.

APPENDIX A

In order to demonstrate that junction line tensions can be negative, we derive an expression for the line tension of a trijunction in soap froth using simple and well-known capillary relations. We compare the capillary forces of an actual trijunction (called a *wet junction*), filled with liquid as shown in Fig. 6, with what there would be if the soap films were mathematical surfaces that continued and met along a trijunction line. We term the comparison junction the *dry junction*. There is no physical trijunction line in the junction and therefore we need to consider only classical capillary forces from the surfaces. We take the line tension of the wet trijunction region to be the difference between the actual tension it exerts and that which the comparison system would exert. We begin by computing the forces from the curved triangular region. Let P_0, γ, λ and r represent, respectively, the pressure of vapor, surface energy, thickness of the surface boundary region and the radius of

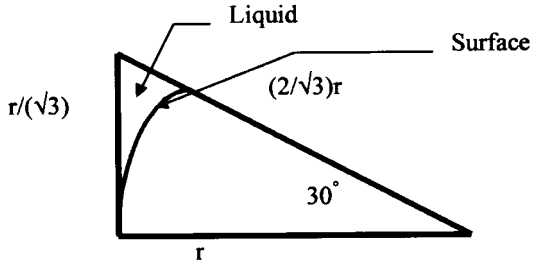

Fig. 7. An illustration of the area relationship between the *dry* soap bubble region and the *wet* trijunction region.

curvature of the film at the trijunction region. The excess pressure inside this curved region is negative, and is given by:

$$\Delta P = \frac{2\gamma}{r} \tag{A1}$$

Consider 1/6th part of this region. We assume the thickness of the surface boundary region λ is negligible compared to "r". There are two forces to consider. One is the direct force from the surface tension of the surfaces. Surface tension is defined as force per unit length of surface. Hence, the product of γ and the arc length in this part ($2\pi r/12$) give us the surface tension force (F_s):

$$F_s = \frac{2\pi r\gamma}{12} \tag{A2}$$

The other force (F_l) is due to the negative pressure and is ΔP multiplied by the cross-sectional area of this part of the region, which is the difference between the areas of the triangle ($r^2/2\sqrt{3}$) and the circular wedge ($\pi r^2/12$),

$$F_l = \frac{\gamma r}{12}(2\sqrt{3} - \pi) \tag{A3}$$

The total tensile force for the wet junction (F_w) is six times the sum of equation (A2) and equation (A3):

$$F_w = \frac{\gamma r}{2}(\pi + 2\sqrt{3}) \tag{A4}$$

Next we see from Fig. 7 that the tensile force from the comparison *dry* junction (F_d) would be entirely from direct surface tension forces from planar surfaces meeting at the trijunction:

$$F_d = \frac{\gamma r}{2}(4\sqrt{3}) \tag{A5}$$

The tension from the comparison junction is larger than from the actual junction. The difference between these forces is the *line tension* (λ_{tj}) and is *negative*:

$$\lambda_{ij} = (F_w - F_d) = -0.161\gamma r \tag{A6}$$

Note that in this model λ_{tj} tends to zero as the liquid volume shrinks to zero.